ELSEVIER

Journal of Nuclear Materials 307–311 (2002) 900–906

journal of nuclear materials

www.elsevier.com/locate/jnucmat

Modeling of void nucleation under cascade damage conditions

H. Trinkaus [a,*], B.N. Singh [b]

[a] *Institut für Festkörperforschung, Forschungszentrum Jülich, Postfach 1913, 52425 Jülich, Germany*
[b] *Materials Research Department, Risø National Laboratory, DK 4000 Roskilde, Denmark*

Abstract

In recent years, significant progress has been made in understanding the void growth and swelling behaviour in metals under cascade damage conditions in terms of differences in the intra-cascade clustering of self-interstitials (SIAs) and vacancies, and the thermal stability and (one-dimensional) mobility of the resulting clusters. The problem of void nucleation was, however, not treated in any detail within this 'production bias model'. In treating void nucleation, the following experimental findings have to be considered: (1) Both nucleation and growth of voids are much more efficient under cascade damage conditions than under electron irradiation. (2) Void nucleation occurs at low dose, particularly in pure metals, and tends to saturate at higher doses. (3) There are significant differences in the void nucleation behaviour between pure metals of different crystal structure and between pure metals and alloys. In the present contribution, we discuss these findings in terms of a production bias controlled vacancy supersaturation rising in the transient to quasi-steady-state and falling during cascade damage accumulation, and thus inducing a limited void nucleation pulse, the yield of which represents the experimentally observed saturated void density.

1. Introduction

In the early 1970s, soon after its discovery [1], void swelling in metals under neutron irradiation was attributed to the preferential absorption of self-interstitial atoms (SIAs) by dislocations ('dislocation bias') [2,3]. At about the same time, the problem of void nucleation under an irradiation induced effective vacancy supersaturation (VSS) was considered [4,5]. In this early work, a constant VSS resulting in a constant steady-state void nucleation rate was assumed.

In the 1980s, the attention shifted to the problems of nucleation and growth of bubbles under the production of gas (mainly helium) [6,7] and the transformation of the once formed bubbles to voids under a simultaneous irradiation induced VSS [8,9]. In the problem of bubble nucleation, the reduction of the gas supersaturation and correspondingly, of the bubble nucleation rate by the evolving bubble structure was taken into account [6,7]. Since, in contrast to gas atoms, SIAs and vacancies are non-conserved defects and can annihilate, the treatment of the equivalent effect in the case of void nucleation under a time-dependent effective VSS appeared to be less straightforward.

In recent years, interest focused on the origin of the VSS under cascade damage conditions. It was recognised that the intra-cascade production of thermally stable SIA clusters, in addition to the formation of (thermally unstable) vacancy clusters ('production bias model', (PBM) [10]), would result in a high VSS, particularly when (part of) the SIA clusters are removed by one-dimensional (1-D) diffusional glide to extended sinks such as dislocations and grain boundaries [11–16]. This PBM has succeeded in rationalising striking features in the swelling behaviour of pure metals where the standard 'dislocation bias model' failed: the high overall swelling even at low dislocation densities, the enhanced swelling near grain boundaries [11] and the related grain size effect [15] as well as the recoil energy dependence of such effects [14]. For modeling damage accumulation in technical alloys, general diffusion-reaction kinetics including the disturbed one-dimensional (1-D to 3-D) diffusion of SIA clusters has been formulated recently

---

[*] Corresponding author. Tel.: +49-2461 61 6460; fax: +49-2461 61 2620.

E-mail address: h.trinkaus@fz-juelich.de (H. Trinkaus).

0022-3115/02/$ - see front matter © 2002 Elsevier Science B.V. All rights reserved.
PII: S0022-3115(02)01120-0

[13,17]. However, modeling of swelling within this framework was, so far, restricted to the consideration of void growth for given void densities, while the problem of (time-dependent) void nucleation was not treated in any detail.

In the present contribution, we sketch an advanced treatment of void nucleation by the biased co-precipitation of (non-conserved) SIAs and vacancies [18], in analogy to the treatment of bubble nucleation by the clustering of (conserved) gas atoms [6,7]. Any treatment of void nucleation has to take into account (1) the (leading) contribution of the 'production bias' to the evolution of the effective VSS under cascade damage conditions, (2) the reduction or even termination of the void (bubble) nucleation rate by the evolving microstructure, (3) differences between metals of different crystal structure and between pure metals and alloys concerning the evolution of the VSS and the resulting void nucleation behaviour. Since void nucleation is much more sensitive than void growth to details in the VSS, we must refine our previous description of the VSS by including, for instance, the continuous accumulation of cascade-induced clusters, stacking fault tetrahedra and dislocation loops during irradiation.

2. Classical theory vs. experimental observations

In the original treatment of void nucleation under an irradiation induced effective VSS [4,5], steady-state conditions with constant VSS and correspondingly, constant void nucleation rates were assumed. On the other hand, in most cases, constant void nucleation rates have never been observed and are probably never realised.

2.1. Classical steady-state nucleation

In the present context, it is useful to consider the dependence of the void (bubble) nucleation rate, $\mathrm{d}N_{\mathrm{v(b)}}/\mathrm{d}t$, on the relevant material, external and microstructural parameters for steady-state conditions as assumed in the original void nucleation theories [4,5]. Relevant are (1) material parameters: specific surface free energy, γ, diffusion coefficients of vacancies, v and SIAs, i (gas atoms, g), $D_{\mathrm{v,i(g)}}$ with migration energies $E^{\mathrm{m}}_{\mathrm{v,i(g)}}$, their thermal equilibrium concentrations $c^{\mathrm{eq}}_{\mathrm{v,i,(g)}}$ and the asymmetry in the behaviour of vacancy and SIA type defects characterised by bias factors (sink and production bias, see below); (2) external control parameters: temperature T and defect production rates $G_{\mathrm{v,i(g)}}$; (3) microstructural parameters: sink strengths of the microstructural components for the absorption of mobile defects (total sink strength k^2).

The driving force for void (bubble) nucleation is the effective vacancy (gas) supersaturation. Neglecting a size dependent void bias, we may write this as

$$s = \begin{cases} (D_{\mathrm{v}}c_{\mathrm{v}} - D_{\mathrm{i}}c_{\mathrm{i}})/D_{\mathrm{sd}} & \text{for voids,} \\ c_{\mathrm{g}}/c^{\mathrm{eq}}_{\mathrm{g}} & \text{for bubbles,} \end{cases} \tag{1}$$

where $c_{\mathrm{v,i,(g)}}$ are the actual concentrations of vacancies, SIAs (and gas atoms), respectively and $D_{\mathrm{sd}} = D_{\mathrm{v}}c^{\mathrm{eq}}_{\mathrm{v}}$, is the self-diffusion coefficient. The supersaturation s depends, via $c_{\mathrm{v,i(g)}}$, on the defect production rates $G_{\mathrm{v,i(g)}}$, the total sink strength, k^2, which is assumed here to be constant (even though it depends on dose rate and dose) and on the bias factors (see below).

For illustrating the parameter dependence of the steady-state void nucleation rate, we consider (similar as in Ref. [3]) the expression for the precipitation of conservative defects (gas atoms into bubbles) which has the form

$$\log \mathrm{d}N_{\mathrm{b(v)}}/\mathrm{d}t \simeq -E^{\mathrm{m}}/T - \gamma^3/T^3 \ln^2 s. \tag{2}$$

According to Eq. (2), the parameters relevant for the steady-state nucleation rate, $\mathrm{d}N_{\mathrm{v(b)}}/\mathrm{d}t$, are $E^{\mathrm{m}}_{\mathrm{v,i(g)}}$, T, γ, and the parameters controlling s, i.e., $P_{\mathrm{v,i(g)}}$, k^2 and SIA/vacancy bias factors. $\mathrm{d}N_{\mathrm{v(b)}}/\mathrm{d}t$ depends particularly sensitively on the ratio γ/T, namely exponentially on its third power! Even slight variations in γ and T can lead to changes in $\mathrm{d}N_{\mathrm{v(b)}}/\mathrm{d}t$ by orders of magnitude. In the case of the void nucleation, the trends are similar. For our later discussion of the termination of void (bubble) nucleation in Section 4, the dependence of s and $\mathrm{d}N_{\mathrm{v(b)}}/\mathrm{d}t$ on dose via k^2 is crucial.

In the present context, it is worth noting that a fully quantitative expression corresponding to Eq. (2) would not yield any significant void nucleation at swelling temperatures if tabulated values for γ were used and the VSS were assumed to be solely due to the dislocation bias. Moreover, the dependence of $\mathrm{d}N_{\mathrm{v(b)}}/\mathrm{d}t$ on $E^{\mathrm{m}}_{\mathrm{v,i(g)}}$ and γ according to Eq. (2) is not able to explain the observed significant differences in the nucleation behaviour between metals of different crystal structure (fcc/bcc) [19] or between pure metals and alloys. In Section 3, such differences will be discussed in terms of differences in intra-cascade clustering and cluster properties.

2.2. Experimental observations

At doses where voids (bubbles) can be resolved in transmission electron microscopy (TEM), their densities seem to remain constant, particularly in pure metals, indicating that they have been nucleated at lower doses. Thus, even though TEM is not suited to study the void (bubble) nucleation phase, we can conclude that void (bubble) nucleation rates are strongly time-dependent in the nucleation phase rather than constant as assumed in the classical treatments. Nevertheless, the saturated void (bubble) density represents a key quantity in void (bubble) nucleation.

In Fig. 1, void densities observed in neutron-irradiated Mo (bcc) and Cu (fcc) are plotted vs. homologous temperature, T/T_m [12]. Temperature dependencies of void densities for other bcc metals (Nb, V [20]), including α-Fe [21], are similar to Mo. For the bcc metals, the most striking feature is the appearance of low and high T branches characterised by small and large apparent activation energies, respectively. Similar low and high T branches have been found for bubbles [7]. In both cases, the temperature dependence is strong, particularly in the high T branches, and of Arrhenius type, but it is by far not as strong and certainly not exponential in the third power of $1/T$ as expected according to Eq. (2).

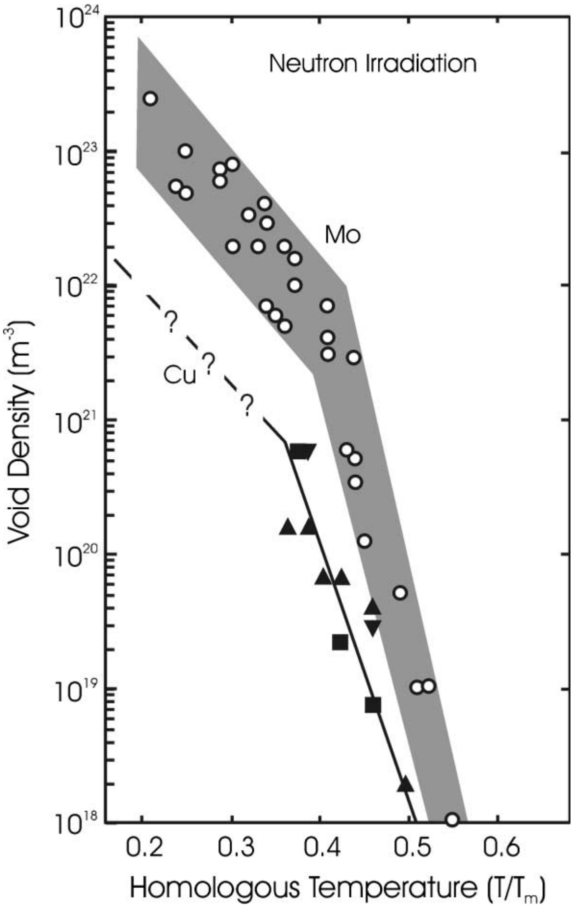

Fig. 1. Temperature dependence of void densities observed in neutron-irradiated Mo and Cu [12].

Apart from these qualitative features, the values of the apparent activation energies, E_a and also of the pre-exponential factors, N_o, characterising the low and high T branches of cavity densities are of interest since these parameters are suited to provide some insight into the character of the nucleation process. Table 1 presents such parameters for bubbles and voids in various types of metals and alloys, obtained by applying Arrhenius type fitting of the form

$$N = N_o \exp(E_a/kT) \tag{3}$$

to experimental data compiled in Refs. [7,12,20]. The activation energies are related to kT_m as well as to the vacancy migration energy, E_v^m and the self-diffusion energy, E_{sd} In spite of rather limited accuracy and substantial scatter, some trends can be clearly recognised. The pre-exponential factors of the low and high T branches differ by about 11–14 orders of magnitude, the former ones ranging between 10^{18} and 10^{21}, the latter between 10^7 and 10^8 m^{-3}. The apparent activation energies of the low and high T branches range from (1.6 to 4)kT_m or (0.25 to 0.6)E_v^m, and from (12 to 18)kT_m or (2/3 to 1)E_{sd} (somewhat higher for bubbles than for voids), respectively. In the first place, the clear separation of the values for the low and high T branches indicate that the mechanisms underlying cavity nucleation at low and high temperatures are qualitatively different, and secondly, the values of the low and high T activation energies indicate that cavity nucleation at low and high T has to do with vacancy or cavity migration [22] and with vacancy or gas dissociation, respectively (see Section 4).

Table 1
Low and high temperature Arrhenius parameters, N_o and E_a derived from experimental data for cavity densities observed in fcc and bcc metals/alloys (bubbles [7], voids [12,20])

Cavity	Metal		N_o (m^{-3})	E_a/kT_m	E_a/E_v^m	E_a/E_{sd}
Bubbles	Aust. SS	Low T	10^{18}	4	0.57	
		High T	10^7	17.5	2.5	0.9
	Ferr. SS	Low T	2×10^{21}	1.6	0.25	
		High T	3×10^7	17	2.7	1
Void	Cu	Low T	–	–	–	–
		High T	10^8	11.5	1.9	0.66
	Mo (Nb, Va)	Low T	8×10^{19}	1.65	0.31	
		High T	1.5×10^7	14	2.6	0.8

The values of E_a are related to kT_m, the vacancy migration energy, E_v^m, and the self-diffusion energy, E_{sd}.

3. Vacancy supersaturation under cascade damage conditions

Until the 1980s, the effective VSS driving void nucleation and growth was assumed to be due the preferential absorption of SIAs by dislocations (dislocation bias). At the beginning of the 1990s, it was recognised that, under cascade damage conditions, the main contribution to the VSS is due to the intra-cascade production of thermally stable SIA clusters, (part of) which are able to migrate and react by 1-D diffusional glide (production bias [10–16]).

In the last decade, the reaction kinetics of the PBM, which includes reactions of mobile and immobile cascade-induced clusters, was developed to a level sufficient to explain some striking features in the void growth and swelling behaviour of pure metals [10–16]. Important features in the complex cluster reaction kinetics, particularly in fcc metals and alloys, are, however, still not fully understood. Thus, in the former version of the PBM, the densities of cascade-induced sessile SIA and vacancy clusters saturate as soon as quasi-steady-state of the mobile point defects is reached [14,16] – in contrast to a continuing, although decelerating density increase of such clusters experimentally observed in pure fcc metals, or even the formation and growth of dislocation loops resulting in network dislocations as observed in alloys. We have to include such features in treating void nucleation since this is much more sensitive to details in the VSS than void growth. The required additional parameters will be deduced from experimental data.

Neglecting, for simplicity, recombination, void bias and second order terms in the dislocation bias, we write the excess vacancy flux defining the VSS in the form

$$\begin{aligned}&(D_\mathrm{v}c_\mathrm{v} - D_\mathrm{i}c_\mathrm{i})(k_\mathrm{v}^2 + \rho)/G_\mathrm{d}\\ &\quad = p_\mathrm{d}\rho/k^2 + \varepsilon_\mathrm{i}^\mathrm{g}(1 - \kappa_\mathrm{c}/\kappa) + (\tilde{\varepsilon}_\mathrm{i}^\mathrm{s} - \tilde{\varepsilon}_\mathrm{v}^\mathrm{s}). \qquad (4)\end{aligned}$$

Here, k_v^2 is the sink strength of the evolving void structure, ρ is the total density of dislocations including the evolving loop structure, k^2 is the total sink strength, $G_\mathrm{d} \approx (0.1G_\mathrm{NRT})$ is the effective generation rate of Frenkel pairs surviving long-term intra-cascade recombination, p_d is a generalized effective dislocation bias including contributions of three-dimensionally migrating SIA clusters, $\varepsilon_\mathrm{i}^\mathrm{g}$ is the effective fraction of SIAs generated in cascades in the form of glissile clusters, κ is the reciprocal mean free path of such clusters within the evolving microstructure, κ_c is the contribution of sessile clusters to κ, and

$$\tilde{\varepsilon}_\mathrm{i,v}^\mathrm{s} = \mathrm{d}n_\mathrm{ic,vc}N_\mathrm{ic,vc}\Omega/\mathrm{d}G_\mathrm{d}t \qquad (5)$$

are the (time-dependent) fractions of SIAs and vacancies deposited continuously by intra-cascade clustering into sessile clusters of (essentially) constant size, respectively (for instance stacking fault tetrahedra, SFTs, in the case of Cu) where $n_\mathrm{ic,vc}$ are the numbers of defects per cluster, $N_\mathrm{ic,vc}$ are the time (dose) dependent number densities of cascade-induced clusters and Ω is the atomic volume. The quantities $\varepsilon_\mathrm{i}^\mathrm{g}$ and $\tilde{\varepsilon}_\mathrm{i,v}^\mathrm{s}$ represent effective cascade parameters, by which the local nature of intra-cascade clustering is taken into account in our kinetic mean field approach. The microstructural parameters k_v^2, ρ, κ_c, κ must be considered to depend on time (dose). In addition, the effective cascade parameters $\tilde{\varepsilon}_\mathrm{i,v}^\mathrm{s}$ given by Eq. (5) must be considered to depend on time via interactions of the corresponding clusters with the evolving microstructure.

The first term on the right hand side of Eq. (4) represents the contribution of the dislocation bias to the VSS, the second and the third ones the glissile and sessile cluster contributions to the production bias. For alloys, cluster diffusion is most likely close to 3-D, because of frequent changes in the 1-D direction induced by impurities [12,13]. In this case, the contributions of mobile SIA clusters may be included into the first term by substituting the single defect dislocation bias p_d by a significantly larger effective cluster dislocation bias, $p_\mathrm{d} \to p_\mathrm{cd}$ [12,13].

Differences in the evolution of the VSS, and by this in the void nucleation behaviour, between metals of different crystal structure (bcc/fcc) [19] or between pure metals and alloys are due to differences in the cascade characteristics, including differences in the properties of clusters [23]. Thus the recombination and the clustering efficiencies are significantly higher in fcc than in bcc metals [24] and the tendency of clusters to form loops and a dislocation network is significantly higher in alloys than in pure metals. This can be taken into account by choosing the above introduced parameters properly. Thus, for bcc, $\tilde{\varepsilon}_\mathrm{i,v}^\mathrm{s}$, κ_c, κ, and the time-dependence of ρ may be neglected; whereas for fcc, $\tilde{\varepsilon}_\mathrm{v}^\mathrm{s}(T,t)$, describing the deposition of vacancies into clusters (SFTs in Cu) must be taken into account. For alloys such as stainless steels (SS), $\varepsilon_\mathrm{i}^\mathrm{g}$ and $\tilde{\varepsilon}_\mathrm{i,v}^\mathrm{s}$ may be neglected whereas the time-dependent total dislocation density $\rho(T,t)$, and an effective cluster dislocation bias p_cd must be taken into account. In this case, however, sufficient and reliable experimental data are only available for the temperature regime of void swelling.

Fig. 2 illustrates the effect of these differences on the dose and temperature dependence of the VSS. Here, we have used for bcc (Mo): $p_\mathrm{d} = 0.02$, $\varepsilon_\mathrm{i}^\mathrm{g} = 0.5$ and $\tilde{\varepsilon}_\mathrm{i,v}^\mathrm{s} = 0$; for fcc Cu: $p_\mathrm{d} = 0.02$, $\varepsilon_\mathrm{i}^\mathrm{g}(= 0.5\varepsilon_\mathrm{i}) = 0.25$ and, $\tilde{\varepsilon}_\mathrm{v}^\mathrm{s}(T,t) \leqslant 0.5$ from experimental data for SFT [25]; for SS: contribution of loops to $\rho(T,t)$ from a large set of experimental data for the swelling regime, and $p_\mathrm{cd} = 0.4$ yielding 1% peak swelling per dpa. For all cases an effective defect generation rate $G_\mathrm{d} = 0.1\ G_\mathrm{NRT} = 10^{-8}$ dpa/s is assumed.

For the three systems considered, the VSS is plotted in Fig. 2(a) vs. NRT-dose for $T = 0.4T_\mathrm{m}$ and various

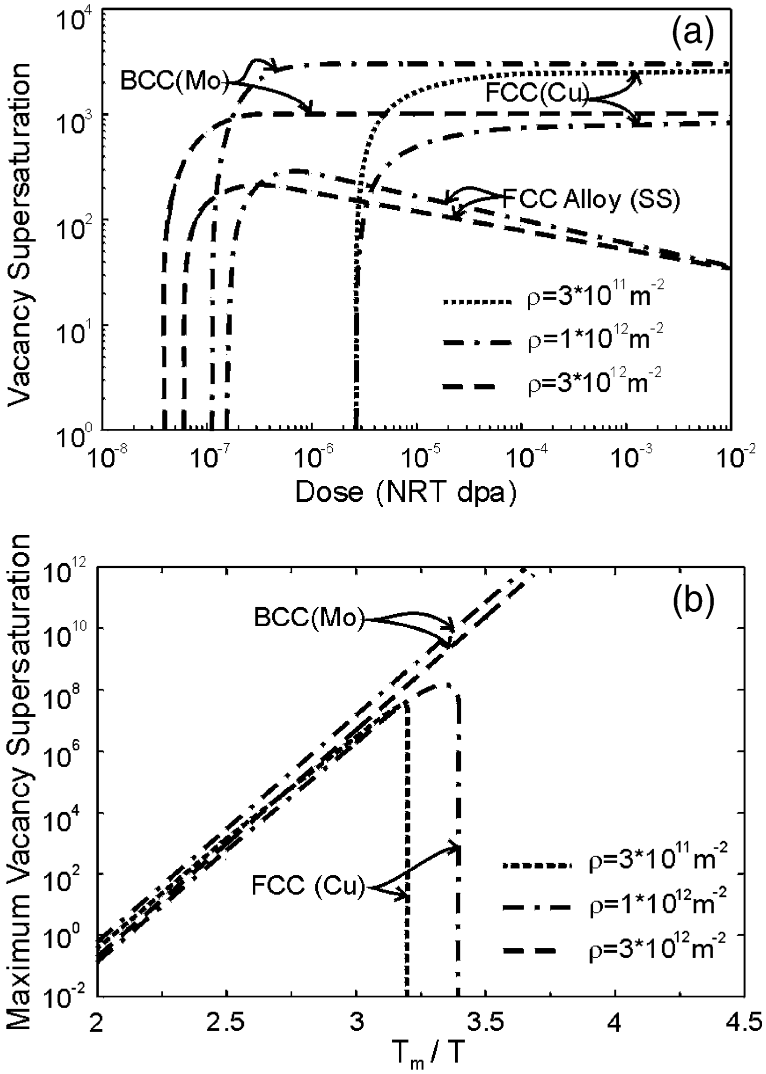

Fig. 2. Calculated trends in (a) dose (b) temperature dependence, respectively, of the VSS induced by neutron irradiation in different types of metals: bcc (Mo), fcc (Cu) and alloys (SS, only in (a)) for $T = 0.4T_m$ and various values of the initial dislocation density. Note the characteristic differences.

values of the initial dislocation density, ignoring the formation of voids, $k_v^2 = 0$. The VSS is negative in the transient to quasi-steady-state. For bcc metals (Mo), the VSS becomes, shortly after quasi-steady-state is reached, very high since virtually all SIA clusters formed are mobile ($\varepsilon_i^g = \varepsilon_i = 0.5$) and no vacancy clusters, other than possibly nano-voids, are formed in cascades ($\tilde{\varepsilon}_v^s = 0$), and it would stay at the high level, if no voids were formed. For Cu, the VSS becomes positive only at doses one order of magnitude higher (some 10^{-6} dpa) because of the initially high value of $\tilde{\varepsilon}_v^s = 0.5$ for SFT, and then increases until the sink strength of the accumulated SFT becomes significant. For SS, the VSS is limited by the build-up of a dislocation loop and network structure, $\rho(T,t)$. In this case, the peak in VSS is too low and too short to yield any significant void nucleation without the assistance of gas, even in well annealed SS with initial dislocation densities as low as 10^{12} m^{-2}. Note that, in this case of sink dominated defect annihilation, the VSS scales with G_d/ρ.

In Fig. 2(b), the maximum VSS for $k_v^2 = 0$ is plotted vs. T_m/T. For bcc metals (Mo), the steep increase in VSS with increasing T_m/T (due to decreasing D_{sd}) in the whole range shown, i.e., even in the low T range, $T_m/T > 3.5$, is consistent with the experimental observation of void formation down to temperatures of $0.2T_m$ (Fig. 1) [12,20]. The sharp cut-off of VSS for Cu at the low temperatures, $T_m/T > 3$, is due to the increase of the

SFT production term $\tilde{\varepsilon}_{\mathrm{v}}^{\mathrm{s}}(t)$ with decreasing temperature according to the experimental data reported in Ref. [25]. Thus, the question marks for Cu in Fig. 1 could be removed: void nucleation is not possible in the low T range, in agreement with recent experiments [26], since the VSS is negative there. For SS, also in the low T range, direct void nucleation without the assistance of gas is unlikely to occur but we cannot parameterise this range because of the lack of experimental data.

We may conclude at this point that the observed differences in the void nucleation behaviour between bcc and fcc metals and between pure metals and alloys can be understood, at least qualitatively, in terms of differences in the evolution of the VSS due to differences in the intra-cascade clustering and properties of the resulting clusters.

4. Modeling cavity nucleation

Generally, the decrease in the vacancy/gas-atom supersaturation associated with the increase in the sink strength during damage accumulation results in a termination of cavity (bubble, void) nucleation. Such a termination may be induced by the accumulation of defects other than cavities (clusters, loops) but for efficient cavity nucleation it will be due to the cavity formation process itself ('self-limitation'). In this section, we sketch an analytical treatment of the 'nucleation yield' of an early peak in the supersaturation.

4.1. Low temperature cavity nucleation

The treatment of bubble nucleation by the clustering of continuously produced but conserved gas (He) atoms is more transparent than that of direct void nucleation by the biased co-precipitation of non-conserved SIAs and vacancies; and the treatment is particularly transparent assuming that already two gas atoms form a stable nucleus [6,7,27]. In this 'di-atomic nucleation' model, which is considered to be representative for the low T branches in cavity nucleation, the maximum nucleation rate is reached when a newly created gas atom is as likely to reach an existing nucleus as to meet another gas atom. The quantitative condition corresponding to this feature yields as an estimate for the number density of bubble nuclei after the nucleation phase, the nucleation yield N_{b} [6,7]:

$$N_{\mathrm{b}} \approx (G_{\mathrm{g}}/\pi r^{*}\Omega D_{\mathrm{g}})^{1/2}, \tag{6}$$

where G_{g} is the gas generation rate and D_{g} is diffusion coefficient (activation energy E_{g}) of the gas atoms, and r^{*} ($\approx$ 1nm) is the trapping radius of a nucleus. For direct void nucleation under a VSS by the reaction of vacancies and SIAs, an expression for N_{v} analogous to Eq. (6) with $G_{\mathrm{g}} \rightarrow G_{\mathrm{d}}$ and $D_{\mathrm{g}} \rightarrow D_{\mathrm{d}}$ can be derived [18].

According to Eq. (6), the low T di-atomic nucleation may be characterised as being diffusion controlled. The apparent activation energy of N_{b} is $E_{\mathrm{a}} = E_{\mathrm{g}}/2$. Considering that $D_{\mathrm{g}} = D_{\mathrm{v}}$ for diffusion of He in metals by the replacement mechanism [6,7], we get for both bubble and void nucleation $E_{\mathrm{a}} = E_{\mathrm{v}}^{\mathrm{m}}/2$, in order of magnitude agreement with the experimental values given in Table 1 for low T. For typical defect generation rates of $G_{\mathrm{d,g}} = 10^{-7}\ \mathrm{s}^{-1}$ for both gas implantation and neutron irradiation, respectively, Eq. (6) yields a pre-exponential factor, N_{o} of about $10^{18}\ \mathrm{m}^{-3}$, again in order of magnitude agreement with the values given in Table 1 for low T. Inclusion of cavity migration by surface diffusion [22] (with diffusion coefficient $\approx D_{\mathrm{v}}$) results in similar values for E_{a} but somewhat reduced values for N_{o} We can conclude that low T cavity nucleation is controlled by the diffusion of the involved point defects and, possibly, small cavities formed by intra- or inter-cascade clustering of vacancies.

4.2. High temperature cavity nucleation

At elevated temperatures ($>0.4T_{\mathrm{m}}$ for voids, $>0.5T_{\mathrm{m}}$ for bubbles), small vacancy (gas atom) clusters can no longer be considered to be thermally stable. Only clusters above some time-dependent critical size are stabilised by further supply of excess vacancies (gas atoms). During the initial build-up of the supersaturation, the critical size first increases, passes a minimum and increases again when the supersaturation is reduced by the evolving cavity structure. The nucleation rate depends now very sensitively on the supersaturation and is, therefore, sharply peaked. In the yield of the nucleation phase, this sensitivity is strongly reduced due to an opposite dependence of the nucleation time, partially compensating the dependence of the supersaturation.

The treatment of this 'self-limiting' cavity nucleation is more complicated in this case than in the low T case, but the approximate results have a similarly simple interpretation. In the present contribution, we can only sketch the procedure. This consists of the following steps: (1) formal definition of the time t^{*} of maximum vacancy (gas atom) supersaturation s and nucleation rate $\mathrm{d}N_{\mathrm{v(b)}}/\mathrm{d}t$, (2) expansion of $\log \mathrm{d}N_{\mathrm{v(b)}}/\mathrm{d}t$ to second order in t around t^{*}, (3) formal integration of the resulting Gaussian expression for $\mathrm{d}N_{\mathrm{v(b)}}/\mathrm{d}t$, giving the yield of the nucleation pulse, (4) self-consistent determination of the coefficients of the Gaussian expansion by demanding that the density of the nuclei at the nucleation peak corresponds to their self-limiting sink strength.

The result for the void (bubble) number density after the nucleation phase, the nucleation yield $N_{\mathrm{v(b)}}$ may be expressed in the simple form

$$N_{\mathrm{v(b)}} \approx G_{\mathrm{d(g)}}/2\pi r^{*} D_{\mathrm{v(g)}} c_{\mathrm{v(g)}}^{*}, \tag{7}$$

where $c^*_{v(g)}$, depending only weakly on the defect generation rate $G_{d,g}$, can be interpreted as the maximum equilibrium vacancy (gas atom) concentration in the presence of critical nuclei of minimum size at $t = t^*$. Since the quantity $D_{v(g)}c^*_{v(g)}$ is a measure for vacancy (gas) dissociation from such critical nuclei, high T cavity nucleation may be called vacancy (gas atom) dissociation controlled. The apparent activation energy of $N_{v(b)}$ is that of $D_{v(g)}c^*_{v(g)}$ which is the energy for the dissociation of vacancies (gas atoms) from critical nuclei, $E^{\mathrm{diss}}_{v(g)}$. For vacancy dissociation, the relation $E^{\mathrm{m}}_{v} < E_{\mathrm{a}} = E^{\mathrm{diss}}_{v} < E_{\mathrm{sd}}$ is obviously fulfilled, in full agreement with the data given in Table 1 for voids. Considering that $D_{\mathrm{g}} = D_{\mathrm{v}}$ and $E^{\mathrm{diss}}_{\mathrm{g}} \geqslant E_{\mathrm{sd}}$ we find a similar relation for bubbles, also in agreement with the data given in Table 1 for bubbles. For typical parameter values, Eq. (7) yields pre-exponential factors of $N_{v(b)}$ between 10^6 and 10^7 m^{-3}, again in reasonable agreement with the data given in Table 1. Thus, we can safely conclude that the high T cavity nucleation is controlled by the dissociation of vacancies (gas atoms) from critical nuclei.

5. Conclusions

In the present contribution, void nucleation under cascade damage conditions has been discussed. The following conclusions can be drawn:

(1) Under cascade damage conditions, the effective VSS driving void nucleation is dominated by the production bias, i.e., by the intra-cascade production of thermally stable and mobile self-interstitial clusters.

(2) Differences in the void nucleation behaviour between pure metals of different crystal structure and between pure metals and alloys can be rationalised in terms of differences in the cascade characteristics and in the properties of defect clusters.

(3) The decrease in the VSS due to damage accumulation causes the termination of void nucleation, as in the case of bubble nucleation. In the case of efficient void (bubble) nucleation, the nucleation process is self-limiting.

(4) An analysis of a nucleation yield of a nucleation phase shows that the low temperature branches in the experimentally observed void (bubble) densities are controlled by the diffusion of vacancies (gas atoms), and possibly small void embryos, whereas the high temperature branches are limited by the dissociation of vacancies (gas atoms) from critical nuclei.

References

[1] C. Cawthorne, E.J. Fulton, Nature 216 (1967) 575.
[2] R. Bullough, B.L. Eyre, R.C. Perrin, Nucl. Appl. Techn. 9 (1970) 346.
[3] S.D. Harkness, Che-Yu Li, Metall. Trans. 2 (1971) 1457.
[4] K.C. Russell, Acta Metall. 19 (1971) 753.
[5] J.L. Katz, H. Wiedersich, J. Chem. Phys. 55 (1971) 1414.
[6] H. Trinkaus, J. Nucl. Mater. 133&134 (1985) 105.
[7] B.N. Singh, H. Trinkaus, J. Nucl. Mater. 186 (1991) 153.
[8] H. Trinkaus, J. Nucl. Mater. 118 (1983) 39.
[9] L.K. Mansur, W.A. Coghlan, J. Nucl. Mater. 119 (1983) 1.
[10] C.H. Woo, B.N. Singh, Philos. Mag. A 65 (1992) 889.
[11] H. Trinkaus, B.N. Singh, A.J.E. Foreman, J. Nucl. Mater. 206 (1993) 200.
[12] S.I. Golubov, B.N. Singh, H. Trinkaus, J. Nucl. Mater. 276 (2000) 78.
[13] H. Trinkaus, B.N. Singh, S.I. Golubov, J. Nucl. Mater. 283–287 (2000) 89.
[14] S.I. Golubov, B.N. Singh, H. Trinkaus, Philos. Mag. A 81 (2001) 2533.
[15] B.N. Singh, M. Eldrup, S.J. Zinkle, S.I. Golubov, Philos. Mag. A 82 (2002) 1137.
[16] B.N. Singh, S.I. Golubov, H. Trinkaus, in: K.H.J. Buschow, R.W. Cahn, M.C. Flemings, B. Ilschner, E.J. Kramer, S.B. Mahalan (Eds.), Encyclopedia of Science & Technology, vol. 8, Pergamon, Oxford, 2001, p. 7957.
[17] H. Trinkaus, H.L. Heinisch, A.V. Barashev, S.I. Golubov, B.N. Singh, Phys. Rev. B 66 (2002) in press.
[18] H. Trinkaus, B.N. Singh, to be published.
[19] B.N. Singh, J.H. Evans, J. Nucl. Mater. 226 (1995) 277.
[20] A.J.E. Foreman, B.N. Singh, in: J. Poirier, J.M. Dupouy (Eds.), Irradiation Behaviour of Metallic Materials for Fast Reactor Core Components, 1979, p. 113.
[21] M. Eldrup, B.N. Singh, S.J. Zinkle, T.S. Byun, K. Farrell, these Proceedings.
[22] B.N. Singh, A.J.E. Foreman, Scrip. Metall. 2 (1975) 1135.
[23] Yu.N. Osetsky, F. Gao, D.J. Bacon, Mater. Res. Soc. Proc. 540 (1999) 691.
[24] Yu.N. Osetsky, A. Serra, B.N. Singh, S.I. Golubov, Philos. Mag. A 80 (2000) 2131.
[25] B.N. Singh, S. Zinkle, J. Nucl. Mater. 206 (1993) 212.
[26] M. Eldrup, B.N. Singh, J. Nucl. Mater. 276 (2000) 269.
[27] G.W. Greenwood, A.J.E. Foreman, E.A. Rimmer, J. Nucl. Mater. 4 (1959) 305.